An Electrostatic MEMS Filament Micromanipulator for Microrobots

Craig B. Schindler, Daniel S. Contreras, Joseph Greenspun, Kristofer S. J. Pister
Berkeley Sensor & Actuator Center
Department of Electrical Engineering and Computer Sciences
University of California, Berkeley
Berkeley, California, USA
Email: {craig.schindler,dscontreras,greenspun,ksjp}@berkeley.edu

***Abstract*—The design and demonstration of a fabricated electrostatic MEMS filament micromanipulator are presented. The device is fabricated using a standard silicon-on-insulator (SOI) MEMS process. A one degree of freedom suspended island containing half of an electrostatic motor can be moved up to 70 μm allowing filaments with diameters of 77 μm or less to be pushed through a channel. The fabricated device is capable of pushing a 7 μm diameter carbon filament through the channel at a speed of 0.2 mm/s. Future applications include a microrobotic spider system as well as a general micromanipulator tool for microrobotic filament, fiber, or wire assembly.**

I. Introduction

Pushup [1], walking [2], jumping [3], and flying [4], [5] microrobots have been demonstrated. Other work has demonstrated microelectromechanical systems (MEMS) capable of creating silicon silk [6], as well as microrobots capable of assembling large diameter (0.48 mm) carbon fibers [7]. However, microrobots capable of manipulating very small diameter filaments, fibers, and wires initially external to themselves is still an area of open research.

We report the results of an electrostatic MEMS filament micromanipulator fabricated using a standard silicon-on-insulator (SOI) process. The SOI wafer used in this process consists of a 40 μm device silicon layer, a 2 μm buried oxide layer, and a 550 μm silicon substrate. The SOI process is shown in Fig. 2. First, the device silicon is patterned and etched using DRIE. Next, the substrate is patterned and etched using DRIE. Finally, a timed vapor HF etch is used to release the structures. The fabricated device is shown in Fig. 1.

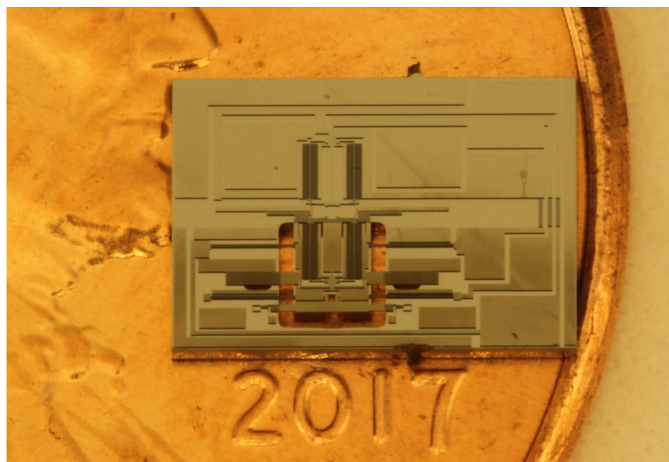

Fig. 1. Photograph of the MEMS filament micromanipulator on a United States penny.

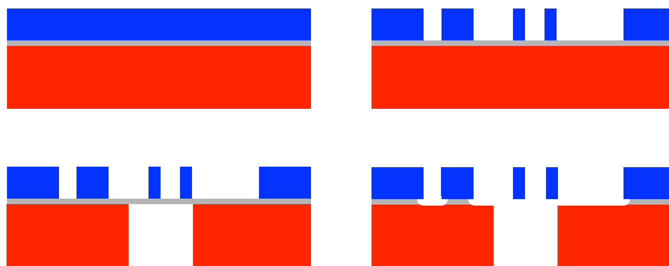

Fig. 2. Cartoon of the SOI process used to make the device. Blue is 40 μm device silicon, gray is 2 μm buried oxide, and red is 550 μm silicon substrate. Top left (step 0): SOI wafer. Top right (step 1): device silicon DRIE. Bottom left (step 2): silicon substrate DRIE. Bottom right (step 3): vapor HF oxide release.

II. Design

Electrostatic motors capable of generating millinewton forces over large distances have been demonstrated [8], [9], [10]. We use the electrostatic motor design from [8] as the force generating actuator for the filament micromanipulator in this paper. The CAD layout of our design is shown in Fig. 3.

The top half of the electrostatic motor contains two electrostatic gap closing actuators and is anchored to the silicon substrate. The bottom half of the electrostatic motor also contains two electrostatic gap closing actuators, but resides on a one degree of freedom island, suspended by four parallel sets of anchored springs. Each set contains five beams, and each beam is 1.2 mm long and 4 μm wide. The suspended island is designed to be moved using a tungsten probe under a microscope (Fig. 4), thereby allowing filaments with different diameters to fit in the motor channel; the suspension springs are designed to withstand up to at least 70 μm of displacement before fracturing [11]. The initial motor channel width is 7 μm, and therefore filaments with diameters of 77 μm or less can fit in the motor channel. Each electrostatic gap closing actuator contains 70 fingers. Each finger has 77 μm of capacitive overlap. The initial front gap of each finger is 5.9 μm, and

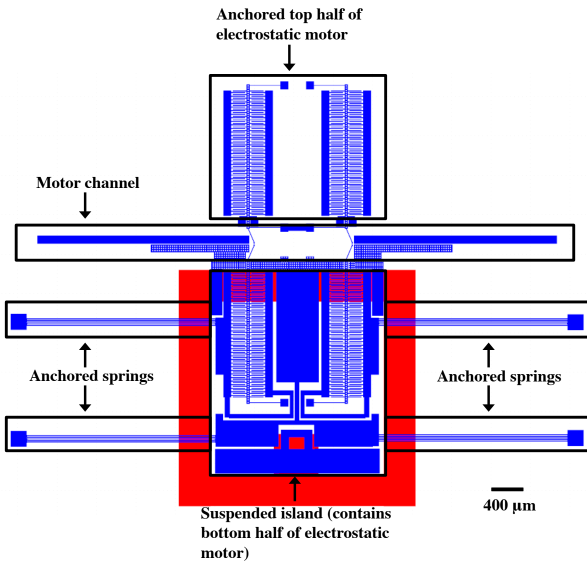

Fig. 3. Layout of the MEMS filament micromanipulator and its various parts. The blue is 40 μm thick device silicon on top of the 550 μm silicon substrate, and the red is a hole cut through the silicon substrate from the back of the wafer.

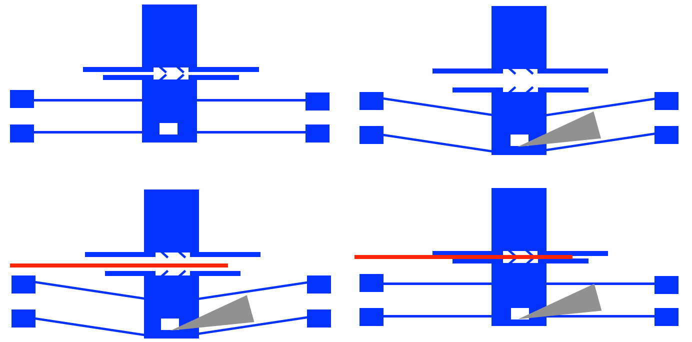

Fig. 4. Cartoon of filament insertion into the micromanipulator. Top left (step 0): Device is in nominal position. Top right (step 1): A tungsten probe tip is used to pull back the island. Bottom left (step 2): The 7 μm carbon filament (shown in red) is inserted into the motor channel. Bottom right (step 3): The motor channel is closed to secure the filament.

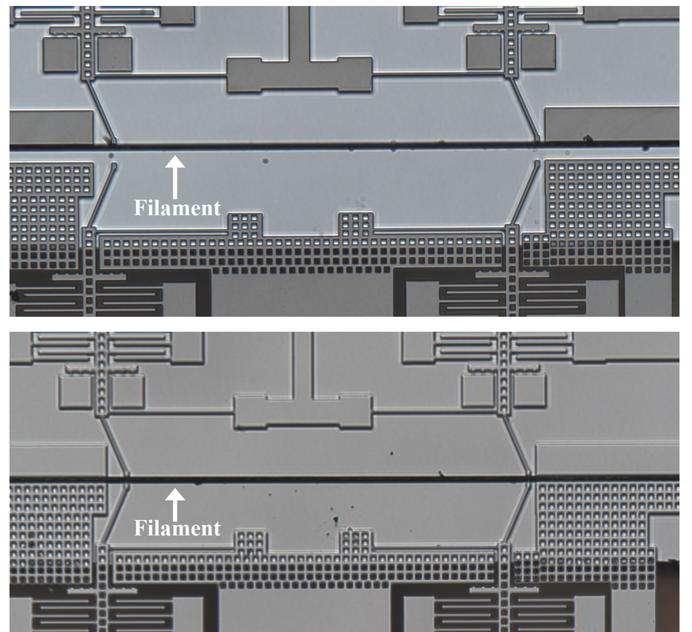

Fig. 5. Top: The suspended island is pulled back by a tungsten probe and the motor channel is opened. A 7 μm diameter carbon filament is inserted into the channel. Bottom: The channel is closed to secure the filament.

the initial back gap is 8.8 μm. Gap stops limit the front gap to a minimum of 1 μm. The movable electrodes' support springs are 195 μm long and 2 μm wide. The motor arms are 93 μm long, 3 μm wide, and angled at 67 degrees. The left electrostatic gap closing actuator on the top half of the motor and the left electrostatic gap closing actuator on the bottom half of the motor are electrically connected, and they therefore actuate simultaneously. This is referred to as the left half of the motor. Likewise, the right electrostatic gap closing actuator on the top half of the motor and the right electrostatic gap closing actuator on the bottom half of the motor are electrically connected, and they therefore actuate simultaneously. This is referred to as the right half of the motor. The left and right halves of the motor are operated in anti-phase such that at least one half is actuated at all times. The filament moves through the motor channel when the motor arms push it.

III. Results

The fabricated MEMS filament micromanipulator shown in Fig. 1 was super glued to a glass slide (Fig. 4, step 0). This glass slide with the super glued device was then placed on a vacuum chuck, and the suspended island containing the bottom half of the device's motor was pulled back with a tungsten probe (Fig. 4, step 1). A piece of an unprocessed SOI wafer was then super glued to a second glass slide. A 7 μm diameter carbon filament was then placed on top of this piece of unprocessed SOI wafer. Finally a third glass slide was placed on top of the carbon filament to prevent it from moving. The stack of the second glass slide, piece of unprocessed SOI wafer, carbon filament, and third glass slide was purposely constructed so that the filament was at the correct height to be inserted into the motor channel. This stack was then carefully placed next to the glass slide on the vacuum chuck, and the filament was inserted into the motor channel of the device (Fig. 4, step 2). Once the filament was successfully inserted into the motor channel, the channel was closed until the motor arms were flush and in contact with the filament (Fig. 4, step 3). Fig. 5 shows steps 2 and 3 using the fabricated device.

Once the 7 μm diameter carbon filament was inserted into the motor channel, the left and right halves of the motor were actuated in anti-phase, each operating at 100 Hz and 70 V. Using this voltage, the theoretical initial electrostatic force produced by each motor half (left and right) at the beginning of every actuation cycle was 0.15 mN [8], [9]. A video taken was subsequently slowed down to capture images of the filament's displacement in 0.5 second intervals. Multiple frames are shown in Fig. 6. A plot of displacement vs. time using the displacement from these frames is shown in Fig. 7.

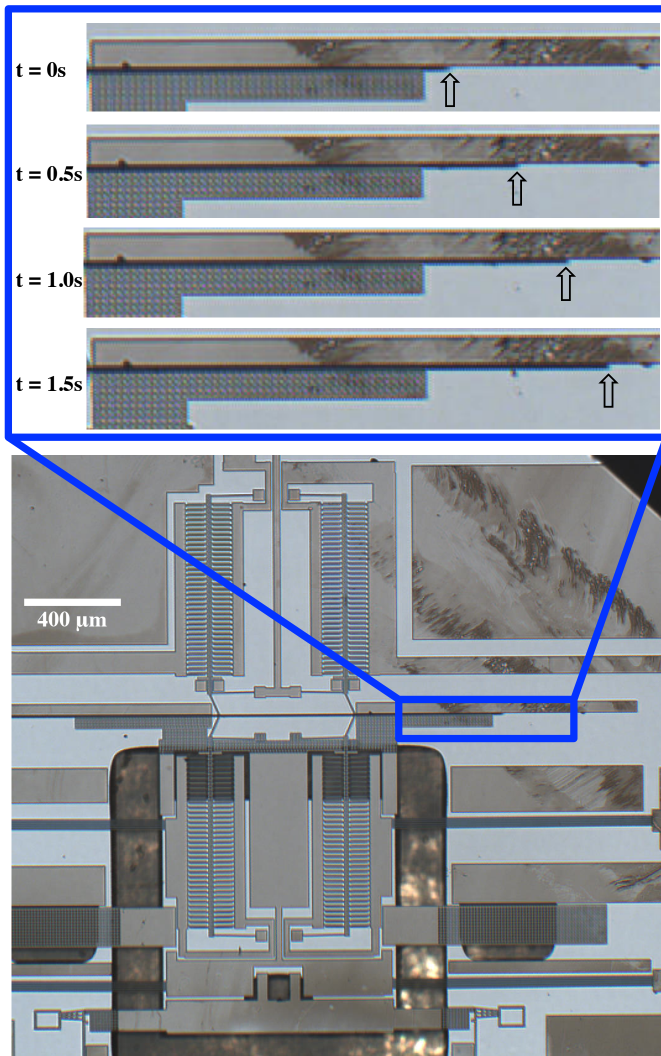

Fig. 6. Multiple frames of a 7 μm diameter carbon filament being pushed through the motor channel. The arrows point to the tip of the filament. The frames show a total displacement of 0.3 mm.

The slope of the line is 0.2 mm/s, which is the fitted speed of filament.

Filament displacement of more than 1.8 mm was achieved; however, after this displacement, a piece of silicon responsible for routing electrical signals to the motor blocked further motion. Future designs will eliminate this issue by using silver epoxy or wire bonding to route electrical signals.

IV. Conclusion

Design and successful demonstration of an electrostatic MEMS filament micromanipulator have been presented. This technology has the potential to be used as a spinneret for a microrobotic spider system capable of climbing a filament. The device presented in this paper weighs 0.27 mN and has less than 1 mm^2 of active motor area (excluding motor periphery). Future designs with motors better optimized for pushing filaments, as well as additional motor area should allow the device to carry not only the weight of the motor, but also of power and control circuits [1]. Additionally, this technology can be used for precision placement of filaments, fibers, or wires during the construction of other microrobots.

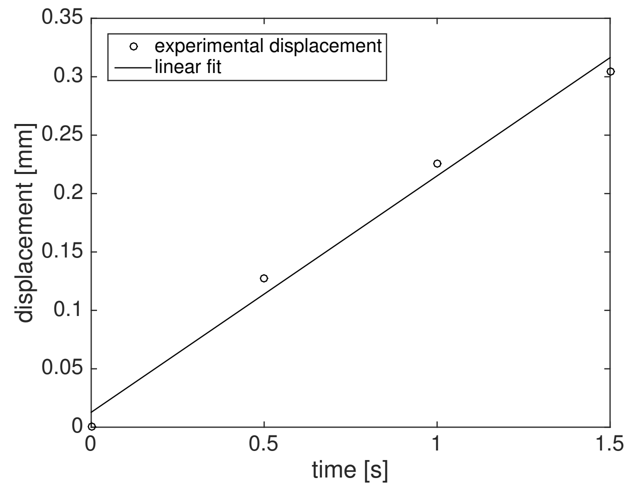

Fig. 7. Experimental displacement vs. time data from Fig. 6. The slope of the linear fit is 0.2 mm/s, which is the fitted speed of the filament.

Acknowledgment

This work is partially supported by the Berkeley Sensor & Actuator Center. All fabrication was performed at the UC Berkeley Marvell Nanolab.

References

[1] S. Hollar, A. Flynn, C. Bellew, and K. Pister, "Solar powered 10 mg silicon robot," in *Micro Electro Mechanical Systems, 2003. MEMS-03 Kyoto. IEEE The Sixteenth Annual International Conference on*. IEEE, 2003, pp. 706–711.

[2] T. Ebefors, J. U. Mattsson, E. Kälvesten, and G. Stemme, "A walking silicon micro-robot," in *Proc. Transducers 99*, 1999, pp. 1202–1205.

[3] S. Bergbreiter and K. S. Pister, "Design of an autonomous jumping microrobot," in *Robotics and Automation, 2007 IEEE International Conference on*. IEEE, 2007, pp. 447–453.

[4] D. Drew, D. S. Contreras, and K. S. Pister, "First thrust from a microfabricated atmospheric ion engine," in *Micro Electro Mechanical Systems (MEMS), 2017 IEEE 30th International Conference on*. IEEE, 2017, pp. 346–349.

[5] R. J. Wood, "The first takeoff of a biologically inspired at-scale robotic insect," *IEEE transactions on robotics*, vol. 24, no. 2, pp. 341–347, 2008.

[6] S. Venkatraman, "Serial assembly of microstructures," Master's thesis, Department of Electrical Engineering and Computer Sciences, University of California at Berkeley, 2006.

[7] A. Hsu, A. Wong-Foy, B. McCoy, C. Cowan, J. Marlow, B. Chavez, T. Kobayashi, D. Shockey, and R. Pelrine, "Application of micro-robots for building carbon fiber trusses," in *Manipulation, Automation and Robotics at Small Scales (MARSS), International Conference on*. IEEE, 2016, pp. 1–6.

[8] I. Penskiy and S. Bergbreiter, "Optimized electrostatic inchworm motors using a flexible driving arm," *Journal of Micromechanics and Microengineering*, vol. 23, no. 1, p. 015018, 2012.

[9] R. Yeh, S. Hollar, and K. S. Pister, "Single mask, large force, and large displacement electrostatic linear inchworm motors," *Journal of Microelectromechanical Systems*, vol. 11, no. 4, pp. 330–336, 2002.

[10] N. Tas, T. Sonnenberg, R. Molenaar, and M. Elwenspoek, "Design, fabrication and testing of laterally driven electrostatic motors employing walking motion and mechanical leverage," *Journal of Micromechanics and Microengineering*, vol. 13, no. 1, p. N6, 2002.

[11] S. D. Senturia, *Microsystem design*. Springer Science & Business Media, 2007.